Journal of General Virology (1997), **78**, 3233–3245. Printed in Great Britain

Biosynthesis, intracellular transport and enzymatic activity of an avian influenza A virus neuraminidase: role of unpaired cysteines and individual oligosaccharides

J. Hausmann,† E. Kretzschmar,‡ W. Garten and H.-D. Klenk

Institut für Virologie, Philipps-Universität Marburg, Postfach 2360, 35011 Marburg, Germany

Intracellular transport, glycosylation, tetramerization and enzymatic activity of the neuraminidase (NA) of fowl plague virus (FPV) were analysed in vertebrate cells after expression from a vaccinia virus vector. Tetramerization occurred with a half-time of 15 min, whereas passage through the medial Golgi apparatus and transport to the plasma membrane occurred with half-times of 2 and 3 h, respectively, suggesting a step in NA maturation beyond tetramerization that limits the rate of transport to the medial Golgi. NA transport rates were about fourfold slower than those of haemagglutinin (HA). Slow transport and processing of FPV NA was not altered by coexpression of FPV HA, nor was the transport rate of HA influenced by NA. The slow transport kinetics of NA were also observed in FPV-infected CV-1 cells. As deduced from the coding sequence, FPV NA has the shortest stalk of all naturally occurring NAs described to date and contains only three potential *N*-glycosylation sites, which are all located in the globular head domain. Elimination of each of the three *N*-glycosylation sites revealed that the two oligosaccharides at positions 124 and 66 are of the complex type, whereas the one at Asn-213 remains in mannose-rich form. The glycosylation mutants showed also that oligosaccharides at positions 124 and 213 of FPV NA modulate enzymatic activity. Transport of NA is not influenced by single elimination of any of the three oligosaccharide attachment sites. Mutational analysis of the three Cys residues not involved in intrachain disulfide pairing revealed that Cys-49 in the stalk of the NA molecule is responsible for the formation of disulfide-linked dimers. Analysis of cysteine mutants of FPV NA also demonstrated that disulfide-linked dimers are not absolutely necessary for the formation of enzymatically active tetramers but may stabilize the quaternary structure of NA.

Introduction

The neuraminidase (NA) of influenza virus is a type 2 membrane glycoprotein with enzymatic activity incorporated into the lipid bilayer of the viral envelope. It hydrolyses the α-ketosidic linkage between terminal sialic acid and the penultimate sugar residue in complex oligosaccharides. Its precise role in the virus life cycle is still not fully understood, but there are data supporting the concept that it plays a role both early and late in infection. Early in infection it may allow the virus to penetrate mucin layers rich in neuraminic acid, which cover the epithelial cells of the respiratory tract (Burnet, 1948). Late in infection, it has been shown to permit release of progeny virus particles from the host cell and to prevent aggregation (Palese *et al.*, 1974). This concept was further supported by the observation that an NA-minus mutant of influenza virus is still infectious but produces progeny virus only in the presence of exogenously added bacterial NA (Liu & Air, 1993). Furthermore, removal of terminal neuraminic acid by viral NA is important for full receptor binding and fusion activity of haemagglutinin (HA) (Ohuchi *et al.*, 1995). Influenza NAs of subtype N9 and also fowl plague virus (FPV) N1 NA display a second biological activity with unknown function which results in binding of erythrocytes (Laver *et al.*, 1984; Hausmann *et al.*, 1995).

Influenza virus NA consists of four major domains, a highly conserved, 6-amino-acid-long cytoplasmic domain, a signal-

Author for correspondence: H.-D. Klenk.
Fax +49 6421 28 8962. e-mail Klenk@mailer.uni-marburg.de

† **Present address:** Abteilung Virologie, Institut für Medizinische Mikrobiologie und Hygiene der Universität Freiburg, Hermann-Herder-Straße 11, 79104 Freiburg, Germany.

‡ **Present address:** Gesellschaft für Transfusionsmedizin, Duisburg mbH, 47051 Duisburg, Germany.

0001-4931

anchor domain of 29 amino acids (Bos *et al.*, 1984), a stalk varying in length between 29 and 45 residues, and a globular head domain carrying the antigenic site and the catalytic centre. The cytoplasmic N terminus of NA seems to play an important role in virus assembly, budding and morphogenesis (Bilsel *et al.*, 1993; Mitnaul *et al.*, 1996; Jin *et al.*, 1997). However, there are also results indicating that the cytoplasmic tail is not essential for particle formation (Garcia-Sastre & Palese, 1995). In virions and infected cells, NA is found as a homotetramer. The three-dimensional structure of the head domain from a number of subtypes including N2, N5, N6, N8 and N9 has been elucidated by X-ray crystallography (Colman *et al.*, 1983; Taylor *et al.*, 1993).

A considerable amount of detailed data about the co- and posttranslational modifications of the influenza virus HA and other type 1 membrane glycoproteins has been accumulated. In contrast, the body of data concerning transport and modifications of influenza virus NA is significantly smaller. Biosynthesis and intracellular routeing of NA begins in the ER where folding and oligomerization take place. The glycoprotein is then transported to the Golgi complex where it is further processed and delivered to the plasma membrane to be incorporated into progeny virions. The stalk of N2 and influenza B virus NA is extensively *N*-glycosylated and is linked to a neighbouring NA stalk of the tetramer by an intermolecular disulfide linkage (Allen *et al.*, 1977; Varghese *et al.*, 1983). It has been postulated that the Cys residues in the stalk might be necessary for stabilization of the stalk and the tetrameric structure of NA (Blok & Air, 1982). Reverse genetic studies performed on the A/WSN/33 strain demonstrated that viruses in which the stalk region had been drastically shortened or completely deleted yielded lower virus titres in certain cell lines or were attenuated in mice (Luo *et al.*, 1993; Castrucci & Kawaoka, 1993). It has not been assessed whether these changes in the growth characteristics of the mutant viruses were due to lack of the stalk as such or loss of the stalk carbohydrates and the conserved Cys residue at position 49, which might be involved in oligomerization of NA.

The present study was performed on NA of influenza virus A/FPV/Rostock/34. We investigated the kinetics of transport and the structural prerequisites for oligomerization, transport competence and full enzymatic activity. In particular, we wanted to clarify the role of oligosaccharide side-chains and of intramolecular disulfide bonds for structure and function of NA. We showed that surface transport of NA is considerably slower than that of HA. Furthermore, we identified oligosaccharide side-chains that modify the enzymatic activity of NA and the Cys residues forming the disulfide bond between NA dimers.

Methods

■ **Cells and viruses.** CV-1 cells were grown in Dulbecco's MEM supplemented with glucose at a high concentration (4·5 g/l) and 5% FCS. Propagation of the WR strain of vaccinia virus in CV-1 was done as described elsewhere (Mackett *et al.*, 1984). Human TK$^-$143 cells were maintained in Dulbecco's MEM supplemented with 5% FCS and 25 μg/ml 5-bromodeoxyuridine (Sigma). Influenza virus A/FPV/Rostock/34 (H7N1) (FPV) was grown on 11-day-old embryonated chicken eggs (Klenk *et al.*, 1972).

■ **Site-directed mutagenesis and construction of recombinant viruses.** Cloning of the cDNA of the NA gene of FPV has been described previously (Hausmann *et al.*, 1995). The cDNA of the NA gene was subcloned in an M13mp18 vector for mutagenesis. Oligonucleotide-directed mutagenesis was carried out according to the method of Taylor *et al.* (1985) with a commercial *in vitro* mutagenesis kit (Amersham) according to the instructions of the manufacturer. Six synthetic oligonucleotide primers were used to create point mutations in the codons for the three Cys residues at positions 14, 49 and 139 in the FPV NA, resulting in codons for Ser residues, and in the codons for the Asn residues in the three sequons for *N*-glycosylation at positions 66, 124 and 213, resulting in codons for Ile or Lys. The mutated NA cDNAs were identified by DNA sequencing using the chain-termination method (Sanger *et al.*, 1977) and mobilized by PCR creating *Bgl*II sites at both ends of the PCR product. After digestion with the respective restriction enzyme, the mutated cDNAs were ligated into the single *Bgl*II site of the pSC11 transfer vector (Chakrabarti *et al.*, 1985). This site was created by insertion of a *Bgl*II linker into the unique *Sma*I site of pSC11. Following subcloning, the DNA sequence of the complete NA cDNA of all constructs was sequenced to verify that only the desired mutations had occurred. Construction of recombinant vaccinia viruses expressing wild-type and mutant NAs was done according to standard procedures using selection by 5-bromodeoxyuridine on TK$^-$143 cells and β-galactosidase expression as has been described in detail previously (Becker *et al.*, 1994).

■ **Infections, labelling and immunoprecipitation.** For labelling and NA activity experiments, about 10^6 CV-1 cells per culture dish were infected at an m.o.i. of 10 with the respective recombinant vaccinia virus and labelled at 3·5–4 h with 100 μCi L-[^{35}S]methionine after a 30 min starvation period for intracellular methionine. Labelling and chase times are given in the legends to the figures for individual experiments. After the indicated chase times, CV-1 cells were lysed in either RIPA buffer [1% Triton X-100, 1% sodium deoxycholate, 0·1% SDS, 0·15 M NaCl, 20 mM Tris–HCl pH 7·8, 10 mM EDTA, 5%, v/v, Trasylol (aprotinin, Bayer), 1 mM PMSF, 10 mM iodoacetamide] or in Triton lysis buffer [1% Triton X-100 in MNT (20 mM MES, 100 mM NaCl, 30 mM Tris–HCl pH 7·5)] supplemented with 1 mM EDTA, 1 mM PMSF, 10 μg/ml pepstatin and 10 μg/ml leupeptin. Insoluble material was pelleted by centrifugation at 14000 r.p.m. for 30 min in an Eppendorf centrifuge at 4 °C. The supernatant was used for immunoprecipitations or chemical cross-linking. All immunoprecipitations of FPV NA were carried out with a polyclonal rabbit antiserum prepared against purified NA heads (Laver, 1978). FPV HA was immunoprecipitated using a monoclonal antibody directed against the HA1 subunit of FPV HA. Immune complexes were recovered using protein A–Sepharose CL-4B (Sigma). Following overnight incubation, protein A–Sepharose-bound immune complexes were washed three times with lysis buffer and once in 20 mM Tris–HCl pH 7·5 prior to dissociation in SDS sample buffer and SDS–PAGE.

■ **Treatment of HA-expressing CV-1 cells with *Vibrio cholerae* NA.** CV-1 cells expressing HA either singly or together with NA due to infection with the respective recombinant vaccinia viruses were pulse-labelled for 15 min at 4 h post-infection (p.i.) After a 1 h chase period, monolayers of 10^6 CV-1 cells were incubated with 0·5 mU *V. cholerae* NA (Behring) for 15 min on ice in 1 ml PBS containing 1 mM $CaCl_2$ and then lysed in RIPA buffer and immunoprecipitated with a monoclonal antibody

directed against the HA1 subunit. The lysates from the coexpressing CV-1 cells were subjected to a second round of immunoprecipitation with the polyclonal anti-NA antiserum.

■ **Endoglycosidase digestion and chemical cross-linking.** Endoglycosidase H (endo H) and endoglycosidase F (endo F)/*N*-glycosidase F (PNGase F) digestions were carried out using immunoprecipitated proteins. The proteins were dissociated from the protein A–Sepharose pellet after the last wash step by incubation in 50 mM sodium phosphate pH 6·5 containing 0·5% β-mercaptoethanol and 0·1% SDS and heated to 95 °C for 5 min. Triton X-100 was added to a final concentration of 0·5% and the protein A–Sepharose was pelleted. Supernatants were divided into three aliquots. The first was left untreated, the second received 1 mU endo H and the third 1 mU endo F. Endoglycosidase digestions were incubated overnight at 37 °C, and the samples were then analysed by SDS–10% PAGE and fluorography. Chemical cross-linking with DSP [dithio-bis(succinimidylpropionate), Pierce] was carried out as described previously (Roberts *et al.*, 1993). Briefly, infected and radioactively labelled CV-1 monolayers were lysed with 0·5 ml Triton lysis buffer (see above) per 10^6 cells. The lysate was cleared by centrifugation and the supernatant was divided into two aliquots. One aliquot was treated with DSP (final concentration 0·32 mM), the other with DMSO to serve as the control. After incubation for 15 min at 15 °C, the reaction was stopped by addition of 1/125 vol. 1 M ammonium hydrogen carbonate and the lysates were subjected to immunoprecipitation as described above. Analysis of oligomeric proteins was carried out by non-reducing SDS–PAGE.

■ **Surface biotinylation of NA.** Monolayers of pulse-chase labelled NA-expressing CV-1 cells in 60 mm culture dishes placed on ice were washed three times with ice-cold PBS containing 0·1 mM $CaCl_2$ and 1 mM $MgCl_2$ (PBS-CM) and then incubated with 2 ml freshly prepared 0·5 mg/ml NHS-SS-biotin [sulfosuccinimidyl-2-(biotinamido)-ethyl-1,3-dithiopropionate, Pierce] in PBS-CM for 30 min on ice. After removal of NHS-SS-biotin solution, the cell monolayer was incubated with Dulbecco's MEM for 3 min to quench unreacted NHS-SS-biotin. Following 3 washes with PBS-CM the cells were lysed in RIPA buffer and subjected to immunoprecipitation with polyclonal anti-NA antiserum and protein A–Sepharose for 16 h as described above. The protein A–Sepharose–immune complex was washed three times with RIPA buffer, resuspended in 20 µl 10% SDS and incubated for 5 min at 95 °C to release the antigen. One ml RIPA buffer was added to the NA suspension and the protein A–Sepharose was pelleted. The supernatant containing immunoprecipitated NA from total cells was incubated for 3 h at 4 °C with streptavidin–agarose (Pierce) to isolate surface NA. The streptavidin–agarose pellet was washed three times with RIPA buffer and processed for endoglycosidase digestion after the last wash step as described above.

■ **Determination of specific NA activity.** To obtain specific NA activities of the cysteine and glycosylation mutants, fetuin was used as a substrate. Lysates of NA-expressing CV-1 cells were prepared in 50 µl PBS and 1/20 vol. of each lysate was used for double assays of NA activity. Reactions were stopped at the indicated time-points between 0 and 90 min and 0 and 150 min, respectively. The liberated sialic acid was quantified by colorimetric assay employing thiobarbituric acid (Aymard-Henry *et al.*, 1973). Results were recorded photometrically by measuring the optical density at 549 nm. To determine specific NA activity of wild-type and mutant NA, cultures of CV-1 cells were infected in parallel with the respective vaccinia viruses and labelled with 20 µCi/ml L-[^{35}S]-methionine from 1·5–5 h p.i. The relative amounts of radioactivity incorporated in the NA-specific bands in SDS–polyacrylamide gels were determined using a PhosphorImager (Molecular Dynamics) and related to the determined enzymatic activities.

Results

Primary structure and expression of FPV NA

cDNA of the FPV NA gene was obtained by RNA PCR and cloned into pUC19 and M13 vectors for sequencing and mutagenesis. The primary structure of the N1 NA of FPV, as deduced from the nucleotide sequence of the cloned gene and confirmed by direct sequencing of the viral RNA, revealed some unusual characteristics. The open reading frame codes for a polypeptide of 447 amino acids, which is very short compared to other influenza virus NAs. This results from a large deletion in the stalk region of the molecule (Fig. 1). The stalk of FPV NA is only 19 amino acids long and is the shortest NA of wild-type strains of influenza virus described to date. Due to this large deletion, most of the potential glycosylation sites known from other influenza A virus NAs are lacking (Fig. 1). Another *N*-glycosylation site found in the stalk of most other influenza virus NAs has been lost due to an amino acid exchange. Thus, FPV NA completely lacks *N*-glycans in the stalk. In the head region, three potential *N*-glycosylation sites are present (Fig. 1) including the highly conserved site at Asn-124.

FPV NA was expressed in CV-1 cells by use of a recombinant vaccinia virus (VV-NA). The expression product was pulse-chase labelled followed by immunoprecipitation. Immunoprecipitated NA was subjected to endo H/PNGase F digestion and the products were analysed by SDS–PAGE. When labelled by a 15 min pulse followed by chase times of up to 6 h, it became clear that FPV NA acquires endo H resistance very slowly (Fig. 2*a*). After a 2 h chase, endo H digestion yielded four bands representing NA with three, two, one or no carbohydrate side-chains. PNGase F treatment confirmed that the smallest form was carbohydrate-free. Without endoglycosidase digestion, a homogeneous 55 kDa polypeptide was observed, which is the theoretical size deduced from the nucleotide sequence of the gene when all *N*-glycosylation sites are used. The endo H digestion pattern therefore indicates that all three potential *N*-glycosylation sites of FPV NA are used. After a 1 h chase period, the majority of NA molecules was still endo H-sensitive, after 2 h of chase there was more endo H-resistant than endo H-sensitive material. Thus, the half-time of transport to the medial Golgi as judged by acquisition of endo H resistance was about 100–120 min. After 6 h of chase there was still some endo H-sensitive material left, demonstrating that not all NA molecules had reached the medial Golgi even after this period of time. The predominant form of NA molecules had two endo H-resistant (i.e. complex) sugars and one high-mannose sugar (Fig. 2*a*, 4–10 h chase). Molecules with all side-chains in the endo H-resistant form (uppermost band) and molecules with one complex and two high-mannose sugars corresponding to the second band (from bottom to top) occurred in roughly equal amounts until 8 h chase time.

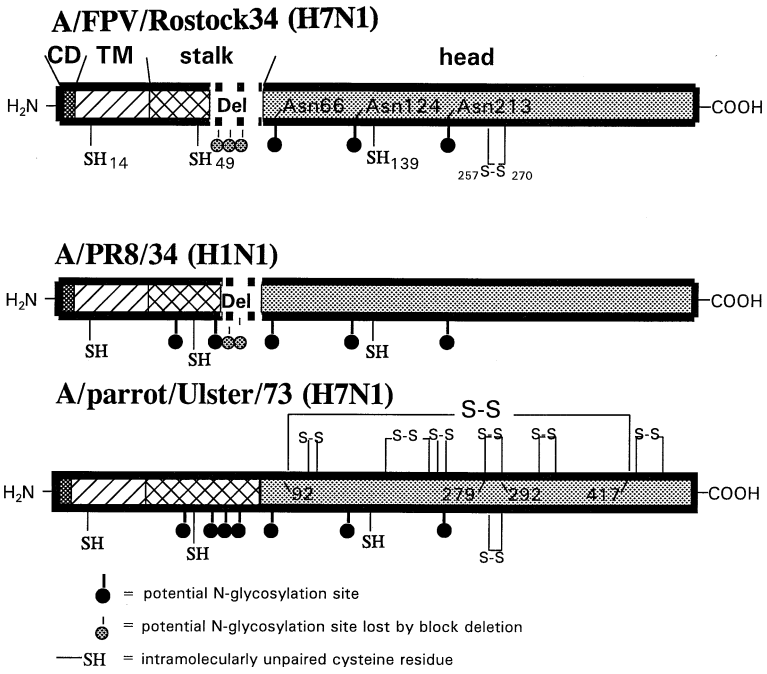

Fig. 1. Schematic representation of the primary structure of FPV NA and two other influenza A virus N1 NAs. The primary structure of FPV NA and the N1 NA from A/PR8/34 and A/parrot/Ulster/73 were deduced from the nucleotide sequence of the corresponding genes. The four domains are represented by different types of shading. The numbers on the representations of FPV NA and A/parrot/Ulster NA refer to amino acid positions in the primary sequence. The intramolecular disulfide bridges and presumably unpaired Cys residues in N1 NA are shown for A/parrot/Ulster, and also apply to FPV NA and A/PR8 NA. Intramolecular disulfide bridging pattern in N1 was deduced by analogy to the disulfide bonds shown for N2 NA. CD, cytoplasmic domain; TM, transmembrane or signal-anchor domain; Del, block deletion.

Analysis of transport kinetics of NA authentically expressed in FPV-infected CV-1 cells confirmed the slow transport of FPV NA. In this system, the conversion of newly synthesized NA into endo H-resistant forms appeared to occur even more slowly (Fig. 2*c*), demonstrating that slow transport of vectorially expressed NA reflects the actual situation in FPV-infected cells. Taken together, these data demonstrate that the low transport and processing rate is an inherent characteristic of FPV NA itself. To confirm that vaccinia virus-expressed NA was functional, we analysed vector-expressed NA and NA present in FPV-infected cells. NA from both sources showed comparable enzymatic activity (data not shown). Thus, functional NA is expressed from the vaccinia virus vector.

Surface expression of FPV NA

The time course of surface expression of FPV NA was also investigated by a pulse-chase approach and subsequent surface biotinylation and endoglycosidase digestion of the surface-exposed NA. For these experiments, a labelling time of 1 h was chosen, followed by various chase times. At the end of each chase period, the surface of the cell monolayers was biotinylated for 15 min on ice prior to lysis and immunoprecipitation of total NA with the monospecific anti-NA antiserum. The biotinylated NA molecules from the cell surface were separated from remaining NA by a second precipitation with streptavidin–agarose. One hour after the beginning of the labelling period, no NA was detectable on the cell surface (Fig. 2*b*, 0 h). After 1 h chase the first weak NA bands appeared, indicating that the earliest time-point of surface expression of FPV NA is about 90 min. The amount of NA on the cell surface increased over the first 8 h and subsequently began to decrease, perhaps because of onset of degradation in the course of plasma membrane turnover (Fig. 2*b*). Biotinylated NA was almost completely resistant to endo H, indicating that mainly the forms with two or three complex oligosaccharides are found at the cell surface. Molecules with completely endo H-sensitive oligosaccharides, or with only one complex carbohydrate, were not biotinylated (see Fig. 2*a*) and therefore represent NA still *en route* to the cell surface.

Coexpression of NA and HA

To investigate interactions between NA and HA during transport and processing, coexpression experiments were carried out. CV-1 cells were coinfected with both recombinant vaccinia viruses, each at an m.o.i. of 5. Pulse-chase labelling followed by immunoprecipitation and endoglycosidase digestion were done as described above. Lysates from co-expressing CV-1 cells were precipitated with a monoclonal antibody against FPV HA in the first round, and the supernatant was then subjected to a second precipitation with the monospecific anti-NA antiserum. Transport and processing of NA were unaffected by coexpression with HA. In particular, no acceleration of the slow transport of NA could be detected (Fig. 3*a*). Similarly, transport of HA, as judged by acquisition of endo H resistance and posttranslational proteolytic cleavage, was not altered by coexpression of NA (Fig. 3*b*, *c*). However, the HA1 subunit coexpressed with NA formed sharper bands and showed increased electrophoretic mobility compared to singly expressed HA (Fig. 3*b*, *c*). This effect was seen more

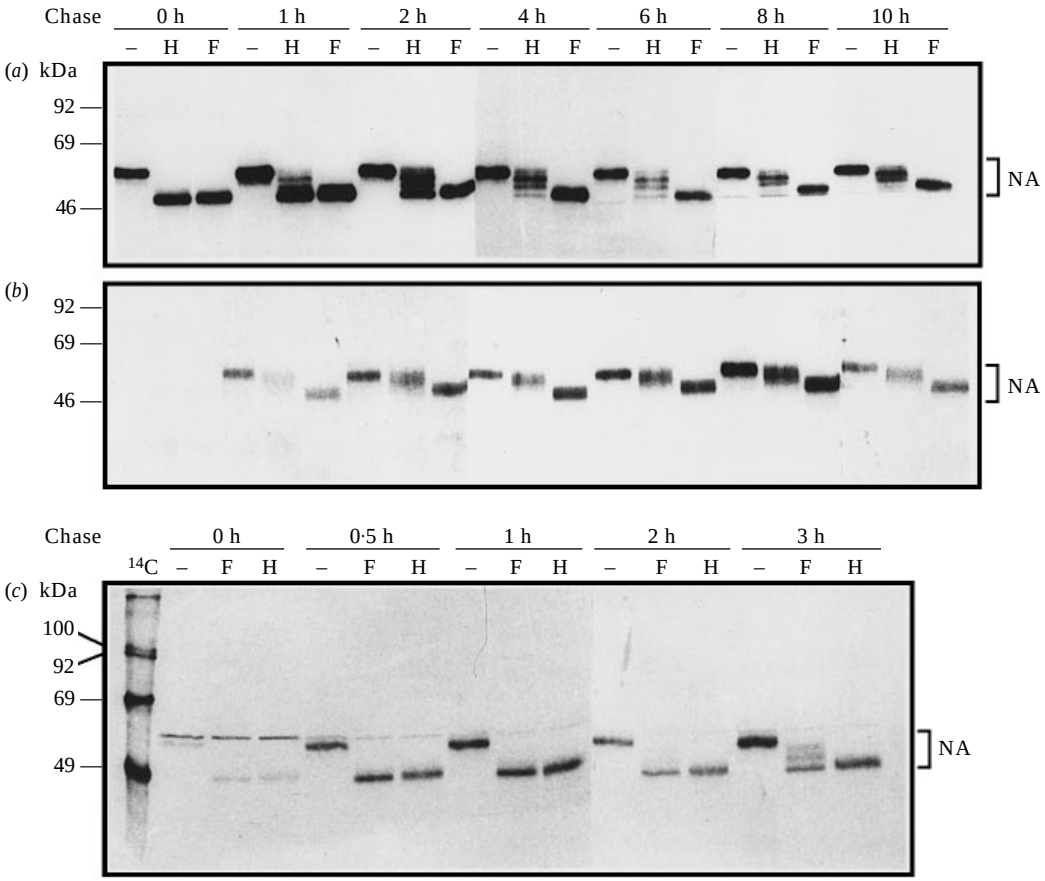

Fig. 2. Kinetics of transport and processing of FPV NA. (*a*) Total NA from CV-1 cells expressing FPV NA. CV-1 cells infected at an m.o.i of 5–10 with recombinant vaccinia virus containing the FPV NA gene were labelled for 15 min with 100 μCi/ml L-[^{35}S]methionine and directly lysed (0 min chase) or chased with 2 mM unlabelled L-methionine for the indicated times. Immunoprecipitation was carried out using monospecific anti-NA antiserum. Immunoprecipitates were subjected to endo H or endo F treatment as indicated and analysed by SDS–10% PAGE and fluorography. (*b*) Analysis of surface-exposed NA. Vaccinia virus-infected CV-1 cells expressing NA were labelled for 60 min with 100 μCi/ml L-[^{35}S]methionine and chased for the indicated times. Following the chase period, NA was biotinylated on the cell surface as described in the text. Surface-exposed NA was then digested with endoglycosidases and analysed by SDS–10% PAGE. (*c*) Total NA from FPV-infected CV-1 cells. Cells were infected with FPV at an m.o.i of 10 and incubated for 5 h, followed by a pulse-chase analysis as in (*a*) with the indicated chase times. ^{14}C, ^{14}C-labelled molecular mass markers.

clearly when HA1 shed into the culture supernatant (Roberts *et al.*, 1993) was compared after single expression and coexpression (Fig. 3*d*). A similar effect was seen when cells expressing HA alone were treated with bacterial NA, but the effect of this external NA on the electrophoretic mobility of surface-exposed HA1 was not as pronounced as that of coexpressed FPV NA (Fig. 3*e*). The electrophoretic mobility of HA1 from NA-coexpressing cells was similar to that of HA1 from FPV-infected CV-1 cells. It is therefore clear that coexpressed NA removes terminal sialic acids from the oligosaccharides of HA.

Oligomerization of FPV NA

Influenza NA is known to form tetramers that consist of two non-covalently associated disulfide-linked dimers. The kinetics of formation of the various oligomeric forms of NA were determined using the pulse-chase approach combined with chemical cross-linking by DSP. Immediately after the 15 min pulse period, two bands of about 55 kDa and 100 kDa molecular mass appeared in non-reducing SDS gels corresponding to the monomeric and the dimeric form of NA, respectively (Fig. 4). The observation that the dimer is detected without prior chemical cross-linking indicates that an intermolecular disulfide bond links the two monomers. The tetrameric form with an apparent molecular mass of 220 kDa is also found in small amounts immediately after the pulse-labelling following cross-linking. The amount of tetramer increased continuously until at least 120 min of chase, whereas the monomeric form almost completely disappeared early after the pulse when treated with the cross-linking reagent (Fig. 4). However, without cross-linking, the amount of monomer did not decrease significantly until at least 4 h of chase, and a

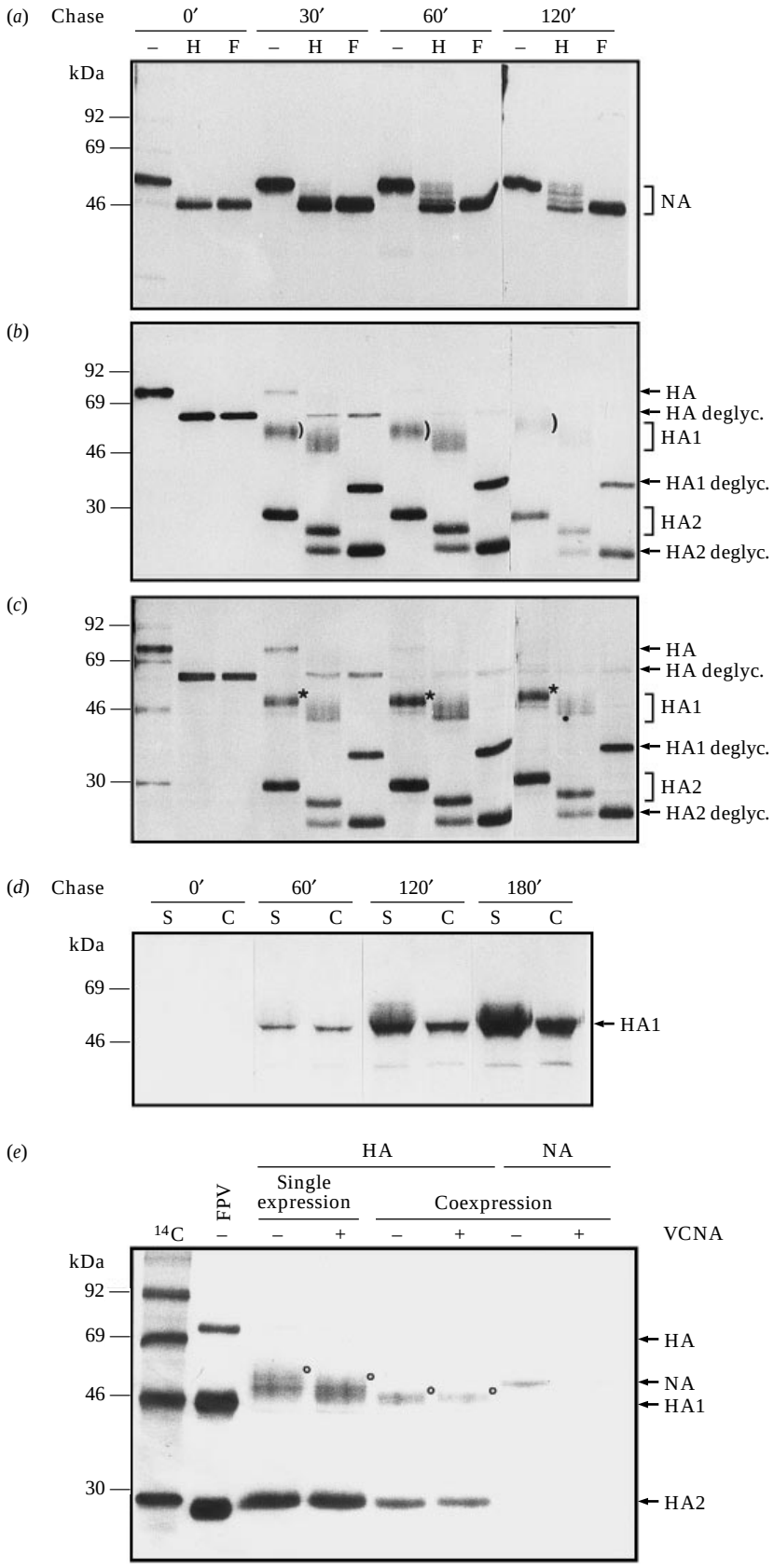

Fig. 3. Coexpression of NA and HA of FPV. CV-1 cells were singly infected at an m.o.i. of 10 with recombinant vaccinia viruses expressing NA and HA, or doubly infected, each at an m.o.i of 5. Cells were labelled with 100 μCi/ml L-[^{35}S]methionine for 15 min and chased for the indicated times with 2 mM unlabelled L-methionine. Cell lysates of coexpressing cells were first immunoprecipitated with a monoclonal antibody against FPV HA1 and then with anti-NA antiserum. Single- and coexpressed HA and NA were then subjected to endo H or endo F digestion and analysed by SDS–PAGE and fluorography. Panel (*a*) shows NA from HA/NA-coexpressing CV-1 cells, (*b*) HA from cells solely expressing HA and (*c*) HA from HA/NA-coexpressing cells. For comparison of coexpressed NA with singly expressed NA, see Fig. 2 (*a*). The round brackets in (*b*) mark diffuse HA1 bands of singly expressed HA; the asterisks in (*c*) mark sharper HA1 bands probably desialylated by coexpressed NA. (*d*) Immunoprecipitation of HA from the supernatant of HA/NA-coexpressing cells by a polyclonal anti-FPV antiserum after the indicated chase times. S, HA singly expressed; C, HA coexpressed with NA. (*e*) Treatment of pulse-chase labelled HA with *V. cholerae* NA (VCNA). CV-1 cells were infected or coinfected with the respective recombinant vaccinia viruses expressing HA and/or NA and were pulse-labelled for 15 min, followed by a 1 h chase. Monolayers of CV-1 cells expressing HA alone or together with NA were incubated with 0·5 mU *V. cholerae* NA for 15 min on ice in PBS containing calcium before lysis and immunoprecipitation with a monoclonal anti-HA1 antibody. Supernatants of the first immunoprecipitation from coexpressing CV-1 cells were subjected to a second immunoprecipitation with anti-NA antiserum (two lanes on far right) to confirm coexpression of NA. The open circles indicate the upper limits of the HA1 bands. FPV, HA expressed by FPV-infected CV-1 cells; ^{14}C, ^{14}C-labelled molecular mass markers. All precipitated proteins were resolved by SDS–10% PAGE and analysed by fluorography.

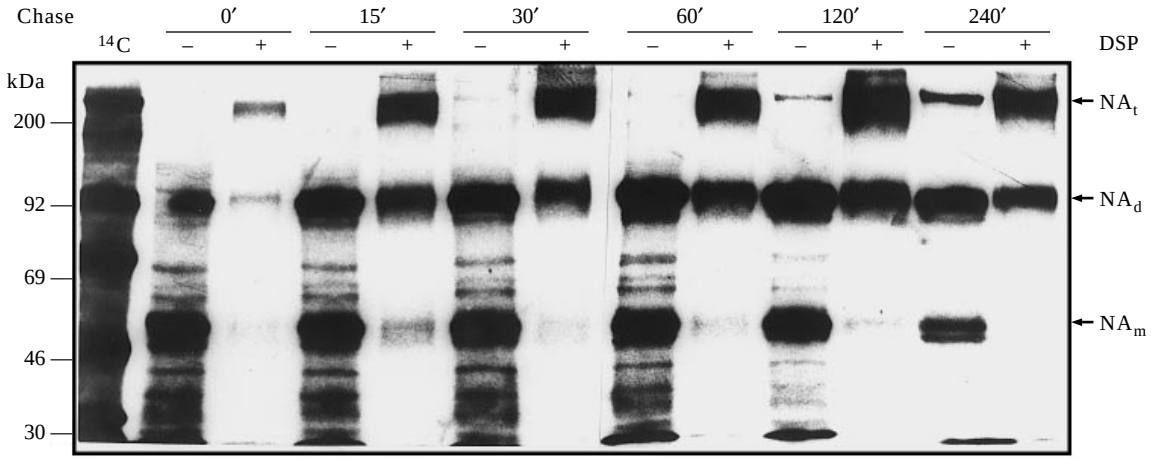

Fig. 4. Kinetics of oligomerization of FPV NA. Infection and pulse-chase labelling were done as described for Fig. 2 (*a*) (15 min pulse). Prior to immunoprecipitation with anti-NA antiserum, cell lysates were divided into two aliquots. One was treated with a 1:125 vol. of a 40 mM solution in DMSO of the synthetic cross-linking reagent DSP (+), the other with DMSO as a control (−). Immunoprecipitated and cross-linked samples were subjected to non-reducing SDS–PAGE (8% acrylamide) and fluorography. The positions of the three oligomeric forms are indicated by NA_t (tetrameric NA), NA_d (dimeric NA) and NA_m (monomeric NA). ^{14}C, ^{14}C-labelled molecular mass markers.

significant portion of monomer still remained after 240 min chase time (Fig. 4). Thus, formation of the intermolecular disulfide bridge appears to be either inefficient or partially reversible. Interestingly, small amounts of a tetrameric form of NA could also be detected in non-reducing SDS–PAGE without prior chemical cross-linking after longer chase times. It is not clear whether this tetramer is stabilized by an additional disulfide bond, but additional modifications in the structure of FPV NA affecting oligomerization apparently occur late after synthesis of the molecule. However, the half-time of tetramerization, as judged after chemical cross-linking, was about 15 min, which is rather fast compared to the slow acquisition of endo H resistance of FPV NA. Concomitant with the late appearance of tetrameric NA without chemical cross-linking, the amount of free monomer began to decrease significantly after 240 min of chase as described above. Thus, oligomerization of FPV NA occurs rather fast with a half-time of about 15 min, but additional changes in the oligomeric structure and possibly folding of NA seem to occur later. In view of the slow acquisition of endo H resistance, these additional modifications may be rate-limiting for export from the ER and thus be responsible for the slow transport of NA through the Golgi apparatus to the cell surface.

Is the disulfide-linked dimer obligatory for tetramerization?

Data from chemical cross-linking experiments indicated that formation of a non-covalently linked dimer occurs significantly faster than formation of the disulfide bridge linking the two subunits of the dimer. This was suggested by the fact that DSP-treated NA showed almost complete dimerization after 15 min of chase whereas without chemical cross-linking a large amount of free monomer was detected until at least 120 min of chase (Fig. 4). In order to identify the Cys residue responsible for the formation of the intermolecular disulfide bond and to determine whether the covalently linked dimer is obligatory for tetramerization and enzymatic activity, we analysed all Cys residues contained in the FPV NA sequence for intrachain pairing by comparison with the reported disulfide bonds in N2 NA (Varghese *et al.*, 1983). Eight of the nine pairs of Cys residues forming intramolecular disulfide bonds in N2 were found to be conserved in FPV NA whereas the remaining three Cys residues were not in positions known to participate in intramolecular disulfide bonds and were therefore assumed to be intramolecularly unpaired (see also Fig. 1). We created three mutants of the FPV NA gene by site-directed mutagenesis. In each of these mutants one of the three unpaired Cys residues was replaced by a Ser residue. The mutants were designated according to the positions of the Cys residues in FPV NA as C14S, C49S and C139S. An additional mutant probably resulted from a random mutation during PCR subcloning of the mutants into the vaccinia virus transfer vector pSC11B. In this mutant, the codon for the Cys-257 (see Fig. 1) was mutated to a Ser codon in addition to the desired exchange of Cys-139 to Ser. This mutant was designated 2C. All other mutants were also sequenced completely to ensure that only the desired mutations were present in the expressed NA mutants.

No dimer or tetramer of mutant C49S could be detected after cross-linking with DSP in non-reducing SDS–PAGE (Fig. 5*a*) after a 1 h labelling period. However, after prolonged chase periods, tetramers of mutant C49S appeared, but in smaller amounts than wild-type NA (Fig. 5*a*). A pulse-chase

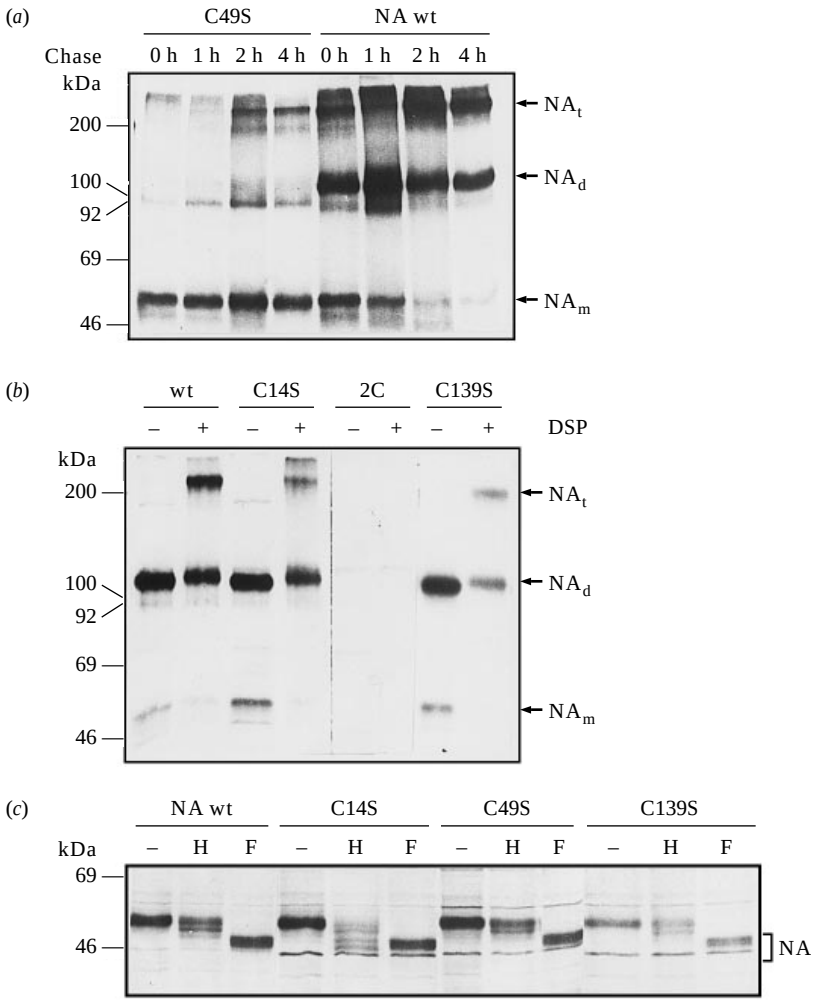

Fig. 5. Oligomerization and transport of cysteine mutants of FPV NA. (*a*) Oligomerization kinetics of wild-type and mutant C49S. CV-1 cells expressing wild-type and mutant C49S were labelled with 50 μCi/ml L-[^{35}S]methionine for 1 h and chased for the indicated times. Immunoprecipitation, subsequent cross-linking by DSP and analysis of proteins by non-reducing SDS–PAGE were performed as described in the legend to Fig. 4. The positions of the three oligomeric forms are indicated by NA$_t$ (tetrameric NA), NA$_d$ (dimeric NA) and NA$_m$ (monomeric NA). (*b*) Oligomerization of NA mutants C14S, C139S and 2C. CV-1 cells expressing wild-type and mutant NAs were labelled for 1 h and chased for another 2 h, followed by immunoprecipitation and DSP cross-linking as described in the legend to Fig. 4. Immunoprecipitates were analysed by non-reducing SDS–PAGE. (*c*) Transport kinetics of cysteine mutants. CV-1 cells expressing wild-type NA or mutants C14S, C49S and C139S were labelled for 1 h and chased for the indicated times. Immunoprecipitation, endoglycosidase digestion and analysis by SDS–10% PAGE were done as described in the legend to Fig. 2 (*a*).

experiment with subsequent chemical cross-linking clearly showed that mutants C14S and C139S were able to form disulfide-linked dimers with similar efficiency to wild-type NA (Fig. 5 *b*). Mutant 2C was not detectable at all after pulse-labelling (Fig. 5 *b*), which might have been due to immediate degradation or by a failure to react with the anti-NA antiserum because of misfolding. This indicates that the intramolecular disulfide bridge between Cys-257 and Cys-270 is essential for correct folding of NA.

In conclusion, the Cys-49 is responsible for intermolecular disulfide bridging but covalently linked dimers are not an absolute requirement for the formation of tetramers. The detectable amount of tetrameric C49S appeared to be smaller than that of wild-type NA (Fig. 5 *a*) and a significant portion of C49S remained in monomeric form even after a 4 h chase whereas almost no monomeric wild-type NA was found after this chase time.

There are two possible explanations for the lower amount of tetrameric mutant C49S: (i) the formation of tetramers is less efficient when no covalently linked dimer is present, or (ii) the tetramer consisting of four non-covalently linked monomers is formed with comparable efficiency but is less stable than the wild-type tetramer and dissociates more easily in the lysis buffer. Reduced stability of the tetramer leading to dissociation into dimers might also be the explanation for a dimeric form of mutant C49S that was often detected in low amounts (Fig. 5 *a*).

Intracellular transport and enzymatic activity of cysteine mutants of FPV NA

The kinetics of transport of C49S to the medial Golgi were similar to those of wild-type NA, as indicated by acquisition of endo H resistance (Fig. 5 *c*). Mutant C139S was also transported with wild-type kinetics, while mutant C14S showed slightly slower rates of transport to the Golgi apparatus. However, all mutants were transported to the cell surface, as demonstrated by indirect immunofluorescence and by surface biotinylation experiments (data not shown). Thus, the incapability of C49S to form covalently linked dimers does not significantly impair surface transport and the mutation in Cys-14 of C14S does not abrogate transport to the cell surface, although it seems to alter transport kinetics. To compare the enzymatic activity of the

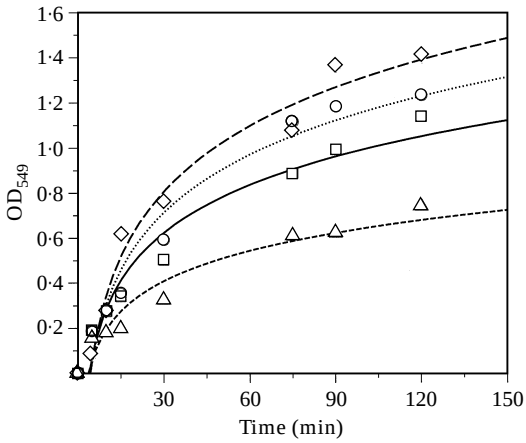

Fig. 6. Specific NA activity of wild-type NA and cysteine mutants of FPV NA. Activity of wild-type NA (□) and cysteine mutants C14S (△), C49S (○) and C139S (◇) was determined using the thiobarbituric acid assay (Aymard-Henry *et al.*, 1973) with fetuin as substrate. CV-1 cells were infected with the respective recombinant vaccinia viruses in parallel sets at an m.o.i. of 10 and incubated for 5 h at 37 °C, after which specific NA activity was measured as described in Methods.

mutants with that of wild-type NA, the specific activity of these NAs in cell lysates was determined. The results of the NA activity assays corresponded with the transport data since mutant C14S also exhibited an impaired enzymatic activity, whereas C139S reached wild-type levels of enzymatic activity (Fig. 6). Interestingly, the NA activity of mutant C49S was completely unaffected by its inability to form disulfide-linked dimers (Fig. 6). Since the detectable amount of tetrameric C49S was lower than that of wild-type NA and the tetramer has to be considered as the correctly folded, transport-competent and enzymatically active form, this finding lends support to the notion that the C49S tetramers are formed with equal efficiency to the wild-type tetramers, but might be less stable under conditions used to detect the tetrameric form by chemical cross-linking.

Influence of individual oligosaccharides on transport and NA activity of FPV NA

To analyse the structural and functional significance of the three *N*-glycans of FPV NA the Asn residues in all three sequons were exchanged for Ile or Lys residues. All three glycosylation mutants had a higher electrophoretic mobility in SDS–PAGE indicating that one of the *N*-glycans is missing (Fig. 7*a*). The glycosylation mutants are transport-competent, as demonstrated by acquisition of endo H resistance of the remaining oligosaccharides (Fig. 7*a*) and by cell surface expression (Fig. 7*b*). It was of particular interest that even the removal of the highly conserved *N*-glycan at Asn-124 did not interfere significantly with transport. From the pattern of endo H digestion, the type of oligosaccharide attached to a specific site can be deduced. Mutant N124I is glycosylated at the two remaining sites as indicated by the electrophoretic mobility of the untreated molecule (Fig. 7*a*), but only one of the two oligosaccharides is resistant to endo H and is hence of the complex type, whereas the other oligosaccharide side-chain remains oligomannosidic, which is clearly seen by endoglycosidase analysis of N124I NA exposed at the cell surface (Fig. 7*b*). There is even a small amount of completely endo H-sensitive N124I on the cell surface. These data indicate that the oligosaccharide at Asn-124 is complex, which was also shown for the respective carbohydrate of N2 NA by biochemical analysis (Ward *et al.*, 1983). When the attachment site at residue 213 was eliminated, endoglycosidase analysis revealed that the resulting mutant (N213K) has two complex oligosaccharides (Fig. 7*a*, *b*). Together with the finding that the majority of wild-type NA molecules have two complex and one oligomannosidic *N*-glycans, this indicates that the carbohydrate at Asn-213 is of the oligomannosidic type. Deletion of the *N*-glycosylation site at Asn-66 leads to a mutant NA (N66I) that is also mainly glycosylated with complex-type sugars as seen with surface-exposed N66I molecules (Fig. 7*a*), but a small proportion of N66I molecules with endo H-sensitive sugars was also detected (Fig. 7*b*), suggesting that a complex-type oligosaccharide is attached to Asn-66. The completely endo H-resistant form of N66I demonstrates that the oligosaccharide at Asn-213 can also be trimmed to a complex-type glycan. This seems to occur more efficiently when Asn-66 is not glycosylated, as suggested by the fact that the majority of the N66I molecules have two complex oligosaccharides. Computer-assisted inspection of the location of both Asn residues on the three-dimensional model of N2 NA reveals that Asn-66 is in the direct vicinity of Asn-213, which probably leads to an interference in trimming of the two oligosaccharides attached to these sites. As the Asn-66 carbohydrate is almost invariably of the complex type in N213K whereas the oligosaccharide at Asn-213 seems to remain untrimmed at least in a small portion of the N66I mutant, we conclude that in wild-type FPV NA the Asn-66 is predominantly glycosylated by a complex sugar. In contrast, the Asn-213 site is probably occupied by an oligomannosidic *N*-glycan in the majority of wild-type NA molecules because of the interference in trimming with the neighbouring oligosaccharide at Asn-66.

When specific enzymatic activities of the glycosylation mutants were analysed, mutant N66I showed wild-type levels of NA activity whereas mutant N124I displayed diminished, but clearly detectable NA activity (Fig. 7*c*). In contrast, previous findings showed that a mutant of N2 NA lacking the corresponding attachment site for an *N*-glycan at position 146 was enzymatically inactive (Lentz *et al.*, 1987). The carbohydrate attachment site at Asn-124 is in the vicinity of the enzyme active site which could explain interference of this oligosaccharide with enzymatic properties of NA. Surprisingly, mutant N213K displayed a more than threefold increase in NA activity (Fig. 7*c*). According to the three-dimensional N2 and

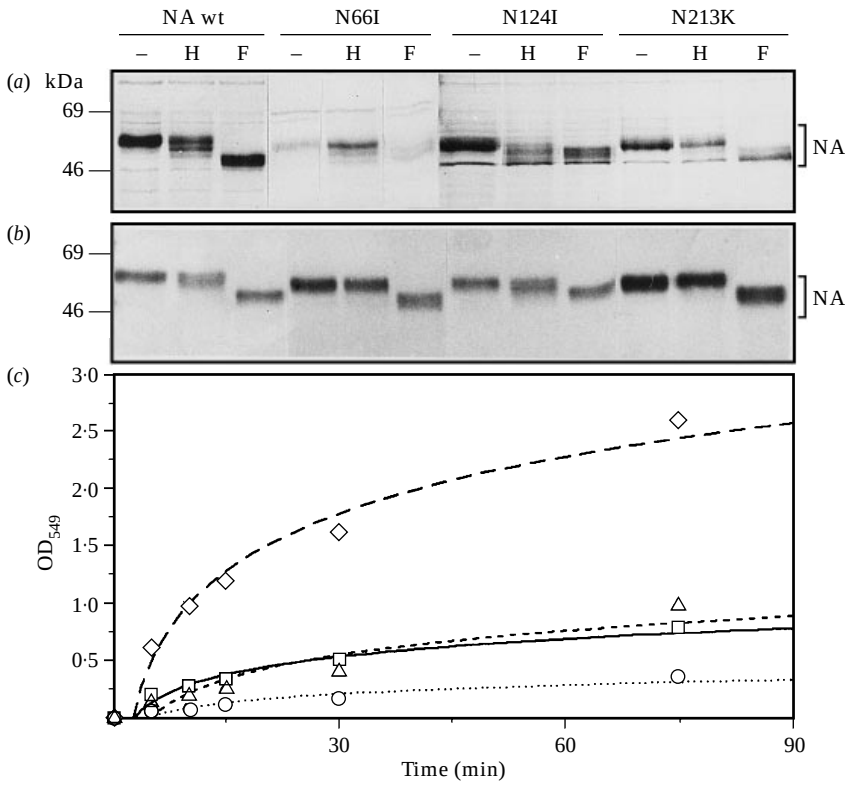

Fig. 7. Processing, transport and enzymatic activity of glycosylation mutants of NA. Total cellular (*a*) and surface (*b*) wild-type NA and glycosylation mutants were analysed by infecting CV-1 cells with the respective recombinant vaccinia viruses at an m.o.i. of 10 and labelling for 1 h with 50 μCi/ml L-[^{35}S]methionine as described in the text, followed by the indicated chase times. Immunoprecipitated wild-type and mutant NAs were digested with endoglycosidases as described and analysed by SDS–10% PAGE and fluorography. (*c*) Specific NA activity of wild-type NA (□) and glycosylation mutants Asn66 (△), Asn124 (○) and Asn213 (◇) were determined as described in Methods. OD_{549} values above 1·0 are due to the normalization of NA activity for expression efficiency.

N9 models, Asn-213 is located far away from the enzyme active centre on the under surface of NA, suggesting an allosteric effect of glycosylation at this site.

The glycosylation mutants of FPV NA demonstrate that the individual oligosaccharides do not play an important role in correct folding, transport and maturation of NA, but that they modulate its biological activity.

Discussion

We describe here the structure and intracellular transport of NA of influenza virus A/FPV/Rostock/34. FPV NA has the shortest stalk of all observed natural influenza virus isolates. It also differs from all other NAs by the lack of *N*-glycans in the stalk. Newly synthesized FPV NA monomers are converted to oligomeric forms with a half-time of 15 min, which is in accordance with the values reported for N8 and N1 NAs (Saito *et al.*, 1995; Hogue & Nayak, 1992). However, further intracellular transport of FPV NA through the exocytotic pathway to the cell surface and maturation of the attached oligosaccharides is rather slow, with a half-time of about 100–120 min for passage through the medial Golgi and about 3 h for transport to the plasma membrane. The transport rate of NA is not affected by coexpressed HA. Mutational analysis revealed that Cys-49 (Cys-78 in N2) in the stalk was responsible for dimer formation via disulfide linkage and that the three individual *N*-glycans do not influence the transport, but modulate the biological activity of NA.

Besides NA, there are several other viral glycoproteins that show slow intracellular transport. The human immunodeficiency virus type 1 gp160 (Earl *et al.*, 1991) and the HN protein of paramyxovirus SV5 (Ng *et al.*, 1989), as well as glycoprotein gB of herpes simplex virus type 1 (Sommer & Courtney, 1991) have five- to eightfold longer half-times of Golgi transport than influenza virus HA. The marked difference between the transport rates of FPV HA, with a half-time of 15–20 min for passage to the medial Golgi and 30 min for transport to the transGolgi network (Fig. 3) on one hand, and NA displaying a half-time of roughly 2 h for transport to the medial Golgi on the other hand, may contribute to the abundance of HA in the viral envelope (Bucher & Palese, 1975). Large differences between the transport rates of two envelope proteins of the same virus have also been observed in the case of the F and HN proteins of Sendai virus (Blumberg *et al.*, 1985; Roux, 1990), where HN is the more slowly transported glycoprotein.

Results obtained on transport of NA from other influenza viruses are somewhat variable, which may be related to expression in different cell types and perhaps also to the expression system. In BHK cells infected with the WSN strain, NA was transported almost as fast as HA (Hogue & Nayak, 1992), whereas in another study in which WSN NA was expressed from a virus vector in CV-1 cells, its transport kinetics resembled those of FPV NA (Kundu *et al.*, 1991). A study addressing the first steps in maturation of N8 NA from synthesis to occurrence of tetramerization in the ER stated a half-time for tetramerization of about 13 min (Saito *et al.*,

1995), which is in good agreement with our data. However, the further transport of the N8 NA through the exocytotic pathway was not investigated in that study.

NA had no effect on transport efficiency of coexpressed HA, but it modified the carbohydrate structures by removal of neuraminic acid. An increase in the receptor-binding activity of HA, as observed after coexpression of NA from simian virus 40 vectors (Ohuchi *et al.*, 1995), could not be clearly recognized. The low receptor-binding activity in the vaccinia virus system may be explained by the relatively high cytopathogenic effect of the vaccinia virus vector and by shedding of HA1 into the medium when using this expression system (Roberts *et al.*, 1993).

Mutational analysis of the *N*-glycosylation sites of FPV NA demonstrated that deletion of single *N*-glycans had no effect on transport efficiency. This is in correspondence with studies on other glycoprotein mutants missing only one carbohydrate (for a review see Doms *et al.*, 1993). A total of two residual carbohydrate side-chains is therefore still sufficient for correct folding and intracellular transport of FPV NA. Moreover, glycosylation in the stalk region is not required for correct folding and oligomerization of FPV NA.

Elimination of the carbohydrate at position 146 in N2 NA, which corresponds to that at position 124 in FPV NA, has been reported to lead to a seriously malfolded NA, as indicated by its transport-defective phenotype (Lentz *et al.*, 1987), whereas the same mutation in FPV NA yielded a transport-competent protein, but with impaired enzymatic activity. Thus, although this oligosaccharide is highly conserved, it does not seem to play a crucial role in folding in all NAs. This conclusion is further supported by results obtained with mutants of WSN NA, which is the only known wild-type NA that is not *N*-glycosylated at this site. Reintroduction of the sugar moiety at this position in the WSN NA altered the enzymatic activity of the mutated NA but not its transport competence (Li *et al.*, 1993).

The cysteine mutants of FPV NA provide direct evidence that Cys-49, the unpaired Cys in the stalk region, is responsible for disulfide-linked dimer formation in influenza virus NA. Our data also show that dimerization by a disulfide bond is not an absolute requirement for tetramerization of the NA, but apparently stabilizes the quaternary structure. Although the detectable amount of tetramer of the C49S mutant was lower in comparison to the wild-type, the specific enzymatic activity was almost identical. These observations are compatible with the finding that stalkless mutants of influenza WSN virus NA are able to form functional tetramers (Castrucci & Kawaoka, 1993). Examples of absence of an absolute requirement for intermolecular disulfide bonds in oligomer formation have also been found by mutational analysis of the cellular transferrin receptor (Alvarez *et al.*, 1989) and the M2 protein of influenza A viruses (Holsinger & Lamb, 1991). The latter study also demonstrated that M2 tetramers lacking interchain disulfide linkages had diminished stability in detergent-containing lysis buffers, which corresponds to our observation that the tetrameric form of mutant C49S is detectable in lower amounts, probably because of reduced stability of the mutant tetramer.

The failure to detect the double cysteine mutant 2C could result from a combination of two effects. Cys-257 is analagous to the Cys-278 residue in N2, which forms a local intramolecular disulfide bond with Cys-291 (Varghese *et al.*, 1983). Cys-291 corresponds to Cys-270 in FPV NA. This intrachain disulfide linkage in a β-sheet portion of the molecule might be crucial for correct folding. The first effect might be lower reactivity of incompletely or improperly folded NA with the antiserum used. Very similar conclusions were drawn from mutational analysis of two non-conserved Cys residues in the HN protein of Newcastle disease virus (McGinnes & Morrison, 1994). This inefficient detection might combine with the second effect, the more rapid degradation of misfolded NA molecules.The phenotype of mutant C14S, with diminished transport efficiency and impaired enzymatic activity, is in agreement with results from mutational analyses aimed at investigating the contribution of the transmembrane region to the targeting and transport of NA. It was shown that a single amino acid substitution in the transmembrane region could heavily impair intracellular transport of WSN NA (Sivasubramanian & Nayak, 1987).

The data presented here show that NA transport is considerably slower than HA transport. There is separate evidence that NA stimulates binding of the M1 matrix protein to membranes and that the stimulatory effect is significantly higher with NA than with HA (Enami & Enami, 1996). These observations taken together lead to the hypothesis that surface transport of NA may be rate-limiting in virion assembly.

We wish to thank Petra Neubauer for expert technical assistance and P.C. Roberts for introduction to the vaccinia virus expression system and providing virus and modified pSC11 vector. This work was done by J. Hausmann in partial fulfillment of the requirements for a PhD degree from the Philipps-Universität, Marburg, Germany, and was supported by the DFG (SFB 286).

References

Allen, A. K., Skehel, J. J. & Yuferov, V. (1977). The amino acid and carbohydrate composition of the neuraminidase of B/Lee/40 influenza virus. *Journal of General Virology* **37**, 625–628.

Alvarez, E., Girones, N. & Davis, R. J. (1989). Intermolecular disulfide bonds are not required for the expression of the dimeric state and functional activity of the transferrin receptor. *EMBO Journal* **8**, 31–40.

Aymard-Henry, M., Coleman, M. T., Dowdle, W. R., Laver, W. G., Schild, G. C. & Webster, R. G. (1973). Influenza virus neuraminidase and neuraminidase inhibition test procedures. *Bulletin of the World Health Organization* **48**, 199–202.

Becker, S., Huppertz, S., Klenk, H.-D. & Feldmann, H. (1994). The nucleoprotein of Marburg virus is phosphorylated. *Journal of General Virology* **75**, 809–818.

Bilsel, P., Castrucci, M. & Kawaoka, Y. (1993). Mutations in the cytoplasmic tail of influenza A virus neuraminidase affect incorporation into virions. *Journal of Virology* **67**, 6762–6767.

Blok, J. & Air, G. M. (1982). Variation in the membrane-insertion and 'stalk' sequences in eight subtypes of influenza type A virus neuraminidase. *Biochemistry* **21**, 4001–4007.

Blumberg, B. M., Giorgi, C., Roux, L., Raju, R., Dowling, P., Chollet, A. & Kolakofsky, D. (1985). Sequence determination of the Sendai virus HN gene and its comparison to the influenza glycoproteins. *Cell* **41**, 269–278.

Bos, T. J., Davis, A. R. & Nayak, D. P. (1984). NH2-terminal hydrophobic region of influenza virus neuraminidase provides the signal function in translocation. *Proceedings of the National Academy of Sciences, USA* **81**, 2327–2331.

Bucher, D. J. & Palese, P. (1975). The biologically active proteins of influenza virus. Neuraminidase. In *Influenza Virus and Influenza*, pp. 83–123. Edited by E. D. Kilbourne. New York: Academic Press.

Burnet, F. M. (1948). Mucins and mucoids in relation to influenza virus action. IV. Inhibition by purified mucoid of infection and haemagglutination with the virus strain WSE. *Australian Journal of Experimental Biology and Medical Science* **26**, 387–391.

Castrucci, M. R. & Kawaoka, Y. (1993). Biologic importance of neuraminidase stalk length in influenza A virus. *Journal of Virology* **67**, 759–764.

Chakrabarti, S., Brechling, K. & Moss, B. (1985). Vaccinia virus expression vector: coexpression of beta-galactosidase provides visual screening of recombinant virus plaques. *Molecular and Cellular Biology* **5**, 3403–3409.

Colman, P. M., Varghese, J. N. & Laver, W. G. (1983). Structure of the catalytic and antigenic sites in influenza virus neuraminidase. *Nature* **303**, 41–44.

Doms, R. W., Lamb, R. A., Rose, J. K. & Helenius, A. (1993). Folding and assembly of viral membrane proteins. *Virology* **193**, 545–562.

Earl, P. L., Moss, B. & Doms, R. W. (1991). Folding, interaction with GRP78-BiP, assembly, and transport of the human immunodeficiency virus type 1 envelope protein. *Journal of Virology* **65**, 2047–2055.

Enami, M. & Enami, K. (1996). Influenza virus hemagglutinin and neuraminidase glycoproteins stimulate the membrane association of the matrix protein. *Journal of Virology* **70**, 6653–6657.

Garcia-Sastre, A. & Palese, P. (1995). The cytoplasmic tail of the neuraminidase protein of influenza A virus does not play an important role in the packaging of this protein into viral envelopes. *Virus Research* **37**, 37–47.

Hausmann, J., Kretzschmar, E., Garten, W. & Klenk, H.-D. (1995). N1 neuraminidase of influenza virus A/FPV/Rostock/34 has haemadsorbing activity. *Journal of General Virology* **76**, 1719–1728.

Hogue, B. G. & Nayak, D. P. (1992). Synthesis and processing of the influenza virus neuraminidase, a type II transmembrane glycoprotein. *Virology* **188**, 510–517.

Holsinger, L. J. & Lamb, R. A. (1991). Influenza virus M2 integral membrane protein is a homotetramer stabilized by formation of disulfide bonds. *Virology* **183**, 32–43.

Jin, H., Leser, G. P., Zhang, I. & Lamb, R. A. (1997). Influenza virus hemagglutinin and neuraminidase cytoplasmic tails control particle shape. *EMBO Journal* **16**, 1236–1247.

Klenk, H.-D., Rott, R. & Becht, H. (1972). On the structure of the influenza virus envelope. *Virology* **47**, 579–591.

Kundu, A., Jabbar, M. A. & Nayak, D. P. (1991). Cell surface transport, oligomerization, and endocytosis of chimeric type II glycoproteins: role of cytoplasmic and anchor domains. *Molecular and Cellular Biology* **11**, 2675–2685.

Laver, W. G. (1978). Crystallization and peptide maps of neuraminidase 'heads' from H2N2 and H3N2 influenza virus strains. *Virology* **86**, 78–87.

Laver, W. G., Colman, P. M., Webster, R. G., Hinshaw, V. S. & Air, G. M. (1984). Influenza virus neuraminidase with hemagglutinin activity. *Virology* **137**, 314–323.

Lentz, M. R., Air, G. M. & Webster, R. G. (1987). Site-directed mutation of the active site of influenza neuraminidase and implications for the catalytic mechanism. *Biochemistry* **26**, 5351–5358.

Li, S., Schulman, J. L., Itamura, S. & Palese, P. (1993). Glycosylation of neuraminidase determines the neurovirulence of influenza A/WSN/33 virus. *Journal of Virology* **67**, 6667–6673.

Liu, C. & Air, G. M. (1993). Selection and characterisation of a neuraminidase-minus mutant of influenza virus and its rescue by cloned neuraminidase genes. *Virology* **194**, 403–407.

Luo, G., Chung, J. & Palese, P. (1993). Alterations of the stalk of the influenza virus neuraminidase: deletions and insertions. *Virus Research* **29**, 141–153.

McGinnes, L. W. & Morrison, T. G. (1994). The role of the individual cysteine residues in the formation of the mature, antigenic HN protein of Newcastle disease virus. *Virology* **200**, 470–483.

Mackett, M., Smith, G. L. & Moss, B. (1984). General method for production and selection of infectious vaccinia virus recombinants expressing foreign genes. *Journal of Virology* **49**, 857–864.

Mitnaul, L. J., Castrucci, M. R., Murti, K. G. & Kawaoka, Y. (1996). The cytoplasmic tail of influenza A virus neuraminidase (NA) affects NA incorporation into virions, virion morphology, and virulence in mice but is not essential for virus replication. *Journal of Virology* **70**, 873–879.

Ng, D. T. W., Randall, R. E. & Lamb, R. A. (1989). Intracellular maturation and transport of the SV5 type II glycoprotein hemagglutinin-neuraminidase: specific and transient association with GRP78-BiP in the endoplasmic reticulum and extensive internalization from the cell surface. *Journal of Cell Biology* **109**, 3273–3289.

Ohuchi, M., Feldmann, A., Ohuchi, R. & Klenk, H.-D. (1995). Neuraminidase is essential for fowl plague hemagglutinin to show hemagglutinating activity. *Virology* **212**, 77–83.

Palese, P., Tobita, K., Ueda, M. & Compans, R. W. (1974). Characterisation of temperature-sensitive influenza virus mutants defective in neuraminidase. *Virology* **61**, 397–410.

Roberts, C., Garten, W. & Klenk, H.-D. (1993). The role of conserved glycosylation in the maturation and transport of the influenza hemagglutinin. *Journal of Virology* **67**, 3048–3060.

Roux, L. (1990). Selective and transient association of Sendai virus HN glycoprotein with BiP. *Virology* **175**, 161–166.

Saito, T., Taylor, G. & Webster, R. G. (1995). Steps in maturation of influenza A virus neuraminidase. *Journal of Virology* **69**, 5011–5017.

Sanger, F., Nicklen, S. & Coulson, A. R. (1977). DNA sequencing with chain-terminating inhibitors. *Proceedings of the National Academy of Sciences, USA* **74**, 5463–5467.

Sivasubramanian, N. & Nayak, D. B. (1987). Mutational analysis of the signal-anchor domain of influenza virus neuraminidase. *Proceedings of the National Academy of Sciences, USA* **84**, 1–5.

Sommer, M. & Courtney, R. J. (1991). Differential rates of processing and transport of herpes simplex virus type 1 glycoproteins gB and gC. *Journal of Virology* **65**, 520–525.

Taylor, G., Garman, E., Webster, R., Saito, T. & Laver, G. (1993). Crystallization and preliminary X-ray studies of influenza A virus neuraminidase of subtypes N5, N6, N8 and N9. *Journal of Molecular Biology* **230**, 345–348.

Taylor, J. W., Ott, J. & Eckstein, F. (1985). The rapid generation of oligonucleotide-directed mutations at high frequency using phosphorothiorate modified DNA. *Nucleic Acids Research* **13**, 8765–8785.

Varghese, J. N., Laver, W. G. & Colman, P. M. (1983). Structure of the influenza virus glycoprotein antigen neuraminidase at 2·9 Å resolution. *Nature* **393**, 35–40.

Ward, C. W., Murray, J. M., Roxburgh, C. M. & Jackson, D. C. (1983). Chemical and antigenic characterisation of the carbohydrate side chains of an Asian (N2) influenza virus neuraminidase. *Virology* **126**, 370–375.

Received 8 May 1997; Accepted 30 July 1997